Continuous galvanizing of martensitic and complex phase steels for automotive anti-intrusion applications

A. Chakraborty, R. Kavitha, J.R. McDermid – McMaster Steel Research Centre, McMaster University, Hamilton, ON, Canada
B. Voyzelle, E. Essadiqi – Materials Technology Laboratory, CANMET, Ottawa, ON, Canada F.E. Goodwin – International Zinc Association, Durham, USA

ABSTRACT

From the perspective of crashworthiness and passenger safety, martensitic and complex phase Ultra High Strength Steels (UHSS) are ideal candidates for automotive anti-intrusion components. However, these steels must be protected from corrosive environments in order to maintain the longterm integrity of the structures involved for which continuous galvanizing is a cost-effective solution. Several challenges have to be overcome in order to process the above steels in the continuous galvanizing line (CGL) while achieving the minimum target tensile strength of 1250 MPa. Steel chemical compositions should be selected in such a way that maintaining a suitable cooling rate produces martensite or bainite, and also provides a substrate surface with sufficient reactive wetting suitable for galvanizing. In the present study, steel chemistries were designed around relatively lean compositions based on carbon, manganese and silicon with additional hardenability being provided by molybdenum or chromium additions. Annealing cycles were determined based on the continuous cooling transformation behaviour of the steels. For both steel compositions the target tensile strength of 1250 MPa was achieved using austenitic annealing for 120s followed by cooling to room temperature at 50°C/s. The steels were successfully reactively wet by the Zn(Al,Fe) bath using a 95%N_2-5%H_2, -30°C dew point process atmosphere. From scanning electron microscopy, X-ray photoelectron spectroscopy and scanning Auger microscopy it was determined that oxides of manganese, silicon and chromium formed during annealing. However, these oxides did not have an adverse effect on coatability and both steels formed high quality, adherent coatings.

RIASSUNTO

Gli acciai a resistenza ultra elevata (UHSS), con struttura formata da martensite e da fasi complesse, sono candidati ideali per realizzare componenti anti-intrusione atti a incrementare la sicurezza dei passeggeri nel caso di scontro frontale di autoveicoli. Per mantenere a lungo la loro integrità strutturale in ambienti aggressivi questi acciai necessitano di un trattamento anticorrosione. A questo fine ben si presta la galvanizzazione continua, che presenta anche il vantaggio di un costo limitato. Per conseguire come obiettivo minimo la resistenza a trazione di 1250 MPa una volta ultimato il processo di galvanizzazione, occorre tuttavia superare diverse difficoltà. La composizione chimica degli acciai va scelta in modo che i) si formi martensite o bainite a seguito di una ragionevole velocità di raffreddamento e ii) la superficie del substrato sia sufficientemente bagnabile, reattiva e quindi adatta alla galvanizzazione. Nel presente studio la chimica dell'acciaio è stata basata su C, Mn e Si con aggiunta di Molibdeno oppure di Cromo per aumentare la durezza. Sono stati definiti cicli di rinvenimento basati sul comportamento dell'acciaio al CCT. Con queste due composizioni dell'acciaio è stato raggiunto l'obiettivo della resistenza tensile di 1250 MPa, adottando il rinvenimento austenitico di 120s seguito da raffreddamento a velocità di 50°C/s fino a temperatura ambiente. Gli acciai sono stati poi immersi in bagno di Zn(Al,Fe) in atmosfera di 95%N_2-5%H_2, con punto di rugiada a -30°C. Le indagini effettuate mediante SEM, spettroscopia fotoelettronica a raggi X e microscopia Auger a scansione hanno messo in evidenza che durante la ricottura si formano ossidi di manganese, silicio e cromo. Non avendo questi ossidi effetti contrari alla formazione di rivestimenti, su ambedue gli acciai si sono ottenuti rivestimenti aderenti e di elevata qualità.

KEYWORDS

Martensitic and complex phase steels; continuous cooling transformation; continuous galvanizing; selective oxidation; reactive wetting.

INTRODUCTION

In order to lower vehicle weight and reduce fuel consumption and undesirable greenhouse gas emissions without deteriorating crashworthiness and passenger safety, the automotive industry is adopting the use of thinner gauge ultra-high strength steels (UHSS) for anti-intrusion components such as side impact door reinforcement beams, bumper beams and roof reinforcements [1]. However, to ensure long-term stability of these structures, these steels must be protected from corrosion, for which continuous hot-dip galvanizing is amongst the most cost-effective solutions. Several challenges have to be overcome in order to process the above steels in the continuous galvanizing line (CGL) without compromising the alloy target tensile strength (>1250 MPa). The challenges are as follows: (a) maintaining a suitable cooling rate to prevent the transformation of austenite to ferrite and pearlite during processing rather than the desired martensite or bainite and, (b) providing a substrate surface which can be reactively wet by the Zn(Al,Fe) CGL bath. Challenge (a) can be addressed by choosing alloy compositions with sufficient hardenability such that martensitic and/or bainitic complex phase microstructures are produced using cooling rates compatible with the CGL. To prevent tempering during isothermal holding while galvanizing at 460°C, the martensite start (M_s) temperature should be lower than 460°C, thereby preventing formation of martensite prior to galvanizing. It is well known that in order to avoid the formation of pearlite, alloying elements such as Mn, Al, Si, Cr, Mo and B can be used [2,3]. These elements shift the continuous cooling transformation (CCT) curves to longer cooling times, such that the desired microstructure can be obtained using a reasonable cooling rate. On the other hand, many of the cited alloying elements will selectively oxidize in commonly employed CGL annealing atmospheres, which can in turn prevent reactive wetting by the CGL bath and result in poor quality coatings. However, this challenge can be addressed by choosing proper alloying elements and a process atmosphere pO_2 which is both cost effective and will produce surfaces with sufficient reactive wetting.

Some open literature is available on the galvanizing of martensitic and complex phase UHSS [4-7], most of which are related to electro-galvanizing or the Quench and Partition process. The present study deals with developing a process window for the galvanizing of a martensitic and/or bainitic complex phase UHSS having a target tensile strength in excess of 1250 MPa. In this investigation two grades of steels were fabricated in the laboratory. The majority of the hardenability of these steels was provided by the C and Mn additions, where Si, Cr or Mo were added to increase the alloy strength and hardenability. The selective oxidation of the alloying elements and their effect on the hot dip galvanizability of the two experimental steels was systematically analyzed to determine a suitable process window for the CGL.

EXPERIMENTAL PROCEDURE

The chemical composition of the experimental steels is shown in Table 1. Except for Mo in steel 1 and Cr in steel 2, the compositions of the steels were quite similar. Experimental steels were fabricated at the Materials Technology Laboratory of CANMET. Alloys were melted in a vacuum induction furnace, cast, hot rolled, pickled, sand blasted and finally cold rolled to a thickness of ~0.9mm. It should be noted that the cooling from the hot rolling step was controlled such that the as-received microstructure for both alloys comprised ferrite and pearlite. The experimental galvanizing heat treatments consisted of austenitic (100% austenite (γ)) annealing for 120s followed by cooling at -50°C/s to the 460°C galvanizing temperature, dipping for 4s and finally cooling to room temperature at 50°C/s. Galvanizing was carried out in an iron saturated Zn-0.18wt.%Al (dissolved) bath maintained at 460°C [8]. The 100% γ formation temperatures and continuous cooling transformation (CCT) diagrams of the experimental steels were determined using a BÄHR-Thermoanalyse quench dilatometer. The peak annealing temperatures for each experimental alloy are reported in Table 2.

All heat treatments and galvanizing experiments were carried out using the McMaster Galvanizing Simulator. Prior to heat treatment, samples were degreased in an 80°C aqueous 2% NaOH solution, rinsed with de-ionized water, cleaned ultrasonically in iso-propanol and dried with warm air. A final cleaning with acetone was performed immediately prior to the sample entering the galvanizing simulator. In the present study, all heat treatments were carried out in the quartz lamp infrared furnace under a 95%N_2-5%H_2 atmosphere with a controlled dew point of -30°C. The sample thermal cycle was controlled using a type K (0.5mm) thermocouple welded directly to the sample before the start of the experiment. Experimental samples comprised 120mm x 200mm panels with the longitudinal axis of the sample parallel to the rolling and dipping directions. A uniform temperature and coating area on the panel of 90mm x 90mm was centred in the lower portion of the steel panel and only material from this area was analyzed.

Table 1. Chemical composition of experimental steels (wt.%).

Sample No.	C	Mn	Si	Al	S	P	Mo	Cr
steel 1	0.16	2.12	0.58	0.01	0.006	0.016	0.11	0.03
steel 2	0.16	2.14	0.57	0.02	0.006	0.017	0.06	0.12

After heat treatment a cross-section of the steel sample was metallographically polished using conventional techniques and etched using 2% nitric acid in ethanol. Microstructural analysis of the sample was performed using a JEOL 7000F field emission scanning electron microscope (FEG SEM). An acceleration voltage of 10keV was used for all samples.

Vickers micro-hardness was measured in a

Table 2. Peak annealing temperatures for experimental steels.

Sample No.	Temperature (°C)
steel 1	862
steel 2	890

Clemex micro-hardness tester using a 200gf load and CMT 5.0 software. Hardness measurements were taken at five different locations for each sample. Tensile testing was performed using an Instron 100kN electro-mechanical load frame with Merlin software. Tensile samples were cut using an abrasive water jet and finish machined using conventional carbide tools to the dimensions outlined in ASTM E 8/E 8M-08 [9] for sub-sized samples with a gage length of 25mm. The sample gage width was 6mm. A constant crosshead speed of 1mm/min was used for all tests. An extensometer was used during tensile testing to measure sample extension.

In order to analyze the selective oxidation of the steel surface, 50mm x 10mm samples were mirror polished to remove surface roughness. Samples were then heat treated without galvanizing and stored in anhydrous iso-propanol to minimize further oxidation before SEM, X-ray Photoelectron Spectroscopy (XPS) and Scanning Auger Microscopy (SAM) examination. The effect of annealing heat treatment parameters on selective oxidation and oxide morphology were determined using the JEOL 700F FEG-SEM. An acceleration voltage of 10keV was used for all samples. Samples were sputter coated with gold to avoid sample charging. Chemical analysis of the oxidized steel surfaces was performed by XPS using a PHI Quantera X-ray photoelectron spectroscope with an Al K_α Xray source (Physical Electronics, Chanhassen, MN). The spot size used was 100μm and the take off angle was 45°. All spectra were calibrated using the metallic iron peak position at 706.62eV. The binding energy values obtained were accurate to within ±0.1eV, and the accuracy of the chemical composition measurements was ±5% of the measured value in atomic percent for each element. The binding energy results shown were collected after sputtering with Ar to a depth of approximately 5nm to avoid oxide layers formed during sample handling. Elemental depth profiles were obtained by Ar sputtering followed by XPS analysis of the new surface. Sputtering depth measurements were considered to be accurate to within ±10%.

The correlation between oxide morphology and elemental distribution was studied using SAM and Auger elemental mapping. SAM data was collected using a JEOL JAMP-9500F field emission Auger microprobe. The energy of the primary electron beam was 15keV for all samples. Samples were tilted at 30° towards the Auger electron analyzer and auto-probe tracking was in effect during the collection of elemental maps to eliminate sample drift. Auger elemental maps were collected after Ar sputtering to a depth of 20nm in order to eliminate the effect of oxidation arising from sample handling. The accuracy of the sputtering depth was ±10%.

Steel reactive wetting by the liquid Zn bath was studied by measuring the bare spot area in the galvanized coating. Measurements of any bare spots present on the galvanized panels were performed using a Nikon AZ100M Stereoscope on the 90mm x 90mm uniform coating area. Images were captured using 10x magnification. The bare spot area was measured by manually selecting the bare spot perimeter. The reactive wetting behaviour was also investigated by analyzing the steel/coating interface via SEM. The interfacial layer on the galvanized panels were exposed for SEM analysis by stripping the zinc overlay using: (i) an inhibited 10% H_2SO_4 solution in water, which leaves any Fe–Zn intermetallics as well as the inhibition layer ($Fe_2Al_{5-x}Zn_x$ $0<x<1$) intact and (ii) fuming nitric acid (HNO_3), which removes any pure Zn and Fe–Zn intermetallics, leaving only the Fe-Al interfacial layer intact. Adherence of the coating to the substrate steel was determined using the 180° 'U' bend test per ASTM A 653/A 653M-09 [10]. Flaking of the coating was analyzed using a Nikon AZ100M stereoscope at the top of the 'U' bend sample.

RESULTS AND DISCUSSION

Steel composition plays a vital role in the production of galvanized martensitic and complex phase steel. Alloying elements such as Mn, Si, Mo and Cr improve steel quench-hardenability by concentrating the carbon in austenite, which increases its stability, and aids in the formation of martensite or bainite. On the other hand, except for Mo, these alloying elements will form stable oxides when exposed to typical CGL annealing furnace atmospheres and can prevent reactive wetting by the liquid zinc bath during galvanizing. For these reasons, the steel composition should be chosen in such a way that it produces sufficient quench-hardenability to be compatible with the cooling capabilities of the CGL along with allowing the production of a surface suitable for reactive wetting by the CGL bath.

Figure 1 shows the experimentally determined CCT diagrams for the present steels. Steel microhardness values as a function of cooling rates are appended to the CCT diagram. From this figure it is observed that for both steels the Ms temperatures are well below the galvanizing bath temperatures (460°C). Since the martensitic transformation takes place after galvanizing there is no possibility of tempering the martensite during galvanizing. Figure 1 also shows that in order to achieve the minimum target strength of 1250 MPa, a minimum cooling rate of 50°C/s was required for both steels. As shown by the highlighted cooling curves in Figure 1, the predicted microstructures at this cooling rate for both steels are dominated by bainite and martensite with minor amounts of ferrite.

Austenitic annealing was carried out at 862°C and 890°C for steel 1 and steel 2, respectively. Figure 2 shows the steel microstructures along with their microhardness after completing the specified annealing cycles. In the case of steel 1, the microstructure contains mostly bainite and lath martensite along with minor amounts of ferrite, whereas bainite and lath martensite along with a considerable amount of ferrite was observed in steel 2. As expected, steel 1 showed higher hardness due to the presence of significantly less ferrite in the microstructure.

Representative engineering stress-strain data for the steels are shown in Figure 3. A summary of the tensile results (yield

Table 3. Summary of steel mechanical properties after annealing.

	Strength (MPa)		Elongation (%)	
Sample No.	YS	UTS	Uniform	Total
steel 1	975	1379	4.50	6.07
steel 2	948	1295	5.29	7.22

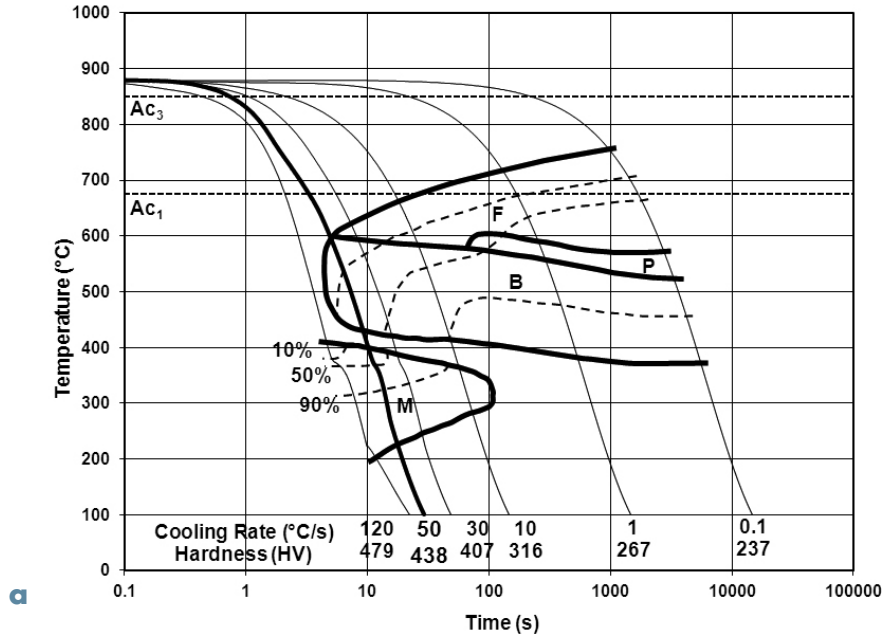

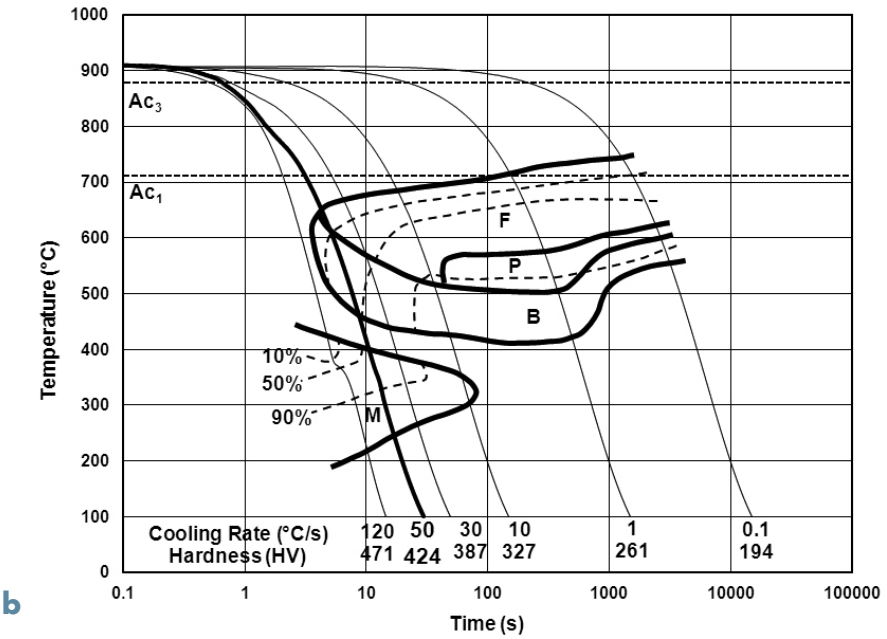

Fig. 1: Continuous cooling transformation diagram of (a) steel 1 and (b) steel 2. (F➜Ferrite, P➜Pearlite, B➜Bainite and M➜Martensite).

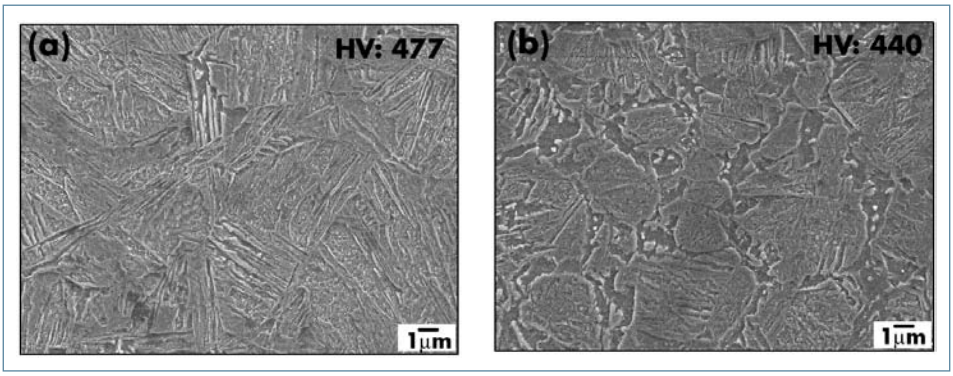

Fig 2: SEM micrographs of steel microstructures after annealing: (a) steel 1, (b) steel 2.

strength (YS), ultimate tensile strength (UTS), uniform and total elongation) for the average of five samples are provided in Table 3. From Figure 3 and Table 3, it can be seen that both steels met the minimum UTS target of 1250 MPa. It was also observed that in steel 1, due to the higher volume fraction of bainite and martensite, there was a significant increase in YS and UTS without a significant deterioration in elongation versus steel 2. From the tensile results, it can also be observed that, when processed using similar cooling rates, the use of Mo in the steel composition produced higher quench hardenability compared to Cr.

Figure 4 shows the SEM microstructures of oxides present on the steel surfaces immediately before galvanizing. For both steels, nodular shaped oxides were distributed over the bulk grain surfaces as well as on the grain boundaries.

Figure 5 shows the chemical composition of the steel surfaces determined via XPS depth profiling. Table 4 lists the binding energies of the elements of interest and the oxide species identified on the steel surfaces. For both steels, considerable surface enrichment of Mn, Si, O and Cr (only for steel 2) was observed, from which it can be concluded that the annealing temperature significantly affected the surface composition as well as the oxides present. It should be noted that no significant surface segregation of Mo was observed for steel 1 (Figure 5(a)). As shown in Figure 5(b), the surface of steel 2, showed a slightly higher level of Mn (~25at.%) compared to steel 1 (~23at.%, Figure 5(a)), whereas a slightly higher amount of Si was observed on steel 1 (~13at.%) compared to steel 2 (~10at.%). On the steel 2 surface, as shown in Figure 5(b), the amount of Cr increased with increasing depth to 30nm, after which it decreased to bulk concentration levels. This could be due to the internal oxidation of Cr.

SAM analysis shows the link between oxide morphology and selective oxidation of the steel alloying elements. Figures 6(a) and 6(b) show the Auger maps for Mn, Si, Mo, Fe and O for steel 1 and Mn, Si, Cr, Fe and O for steel 2, respectively. From Figure 6 it can be observed that during annealing prior to galvanizing, considerable enrichment of Mn and Si (both steels) and Cr (for steel 2) in the form of oxides was present on the steel surfaces. From Figure 6

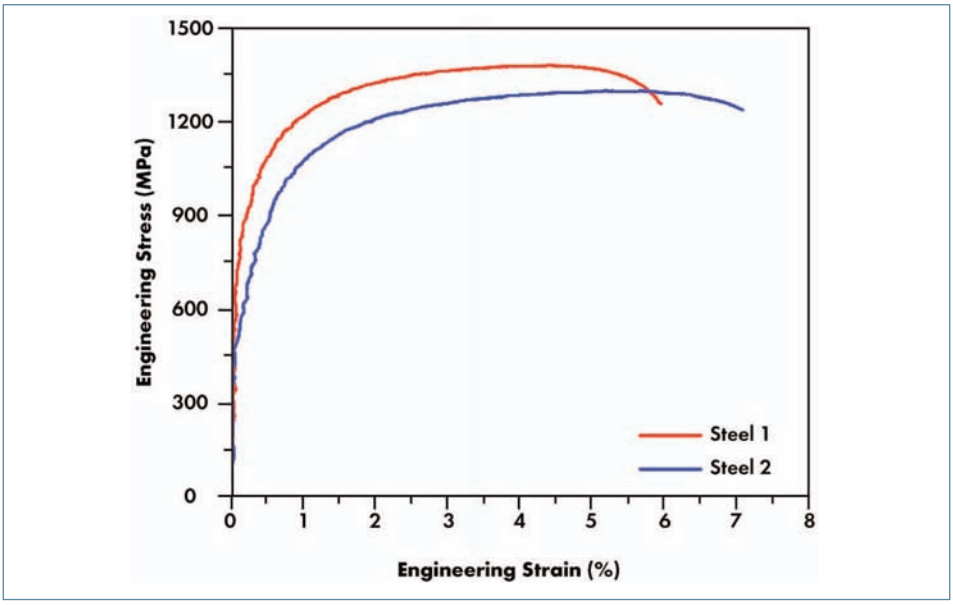

Fig 3: Engineering stress-strain plots for the experimental steels after annealing.

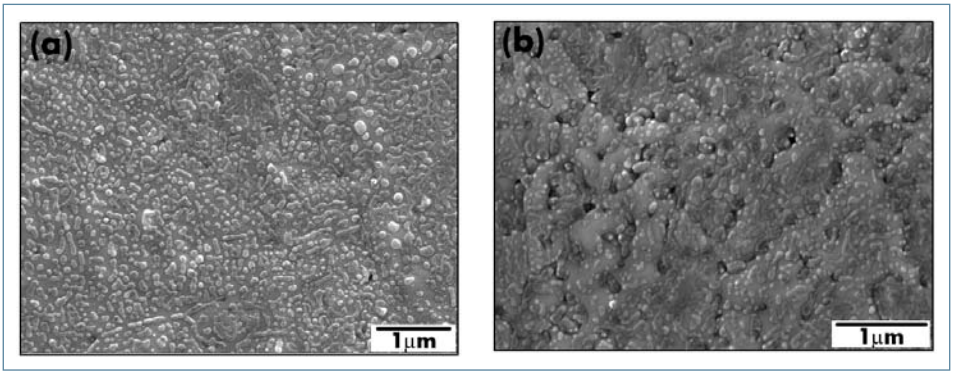

Fig 4: SEM micrographs of the oxides formed on the steel surface during annealing: (a) steel 1 and (b) steel 2.

it can be observed that nodular MnO and mixed (Mn, Si) oxides were distributed over the bulk grain surfaces as well as along the grain boundaries for both steels. Consistent with the XPS observations for steel 1 (Figure 5(a)), there was no surface segregation of Mo observed during the SAM analysis, confirming that under the present annealing process atmosphere Mo-oxides were not formed. On the other hand, on the surface of steel 2, the segregation of Cr-oxides was prominent primarily along the grain boundaries. As there is some correspondence between the Mn, Cr and O maps for steel 2, it is possible that some nodules comprised mixed (Mn,Cr) oxides.

The ability of the zinc bath to reactively wet the steel surface was determined by assessing the population and size of bare spots on the coating and by observing the Fe–Zn interface to determine if any reaction products were present. The area percentages of bare spots and average bare spot size within the uniform coating area are summarized in Table 5. Both steels showed excellent coatability despite the presence of oxides on the surface before galvanizing (Figures 4, 5, 6 and Table 4). This may be the result of in-situ aluminothermic reduction of the surface oxides by bath dissolved aluminum exposing the underlying Fe, thereby allowing reactive wetting to occur [11,12].

Areas of the galvanized panels that

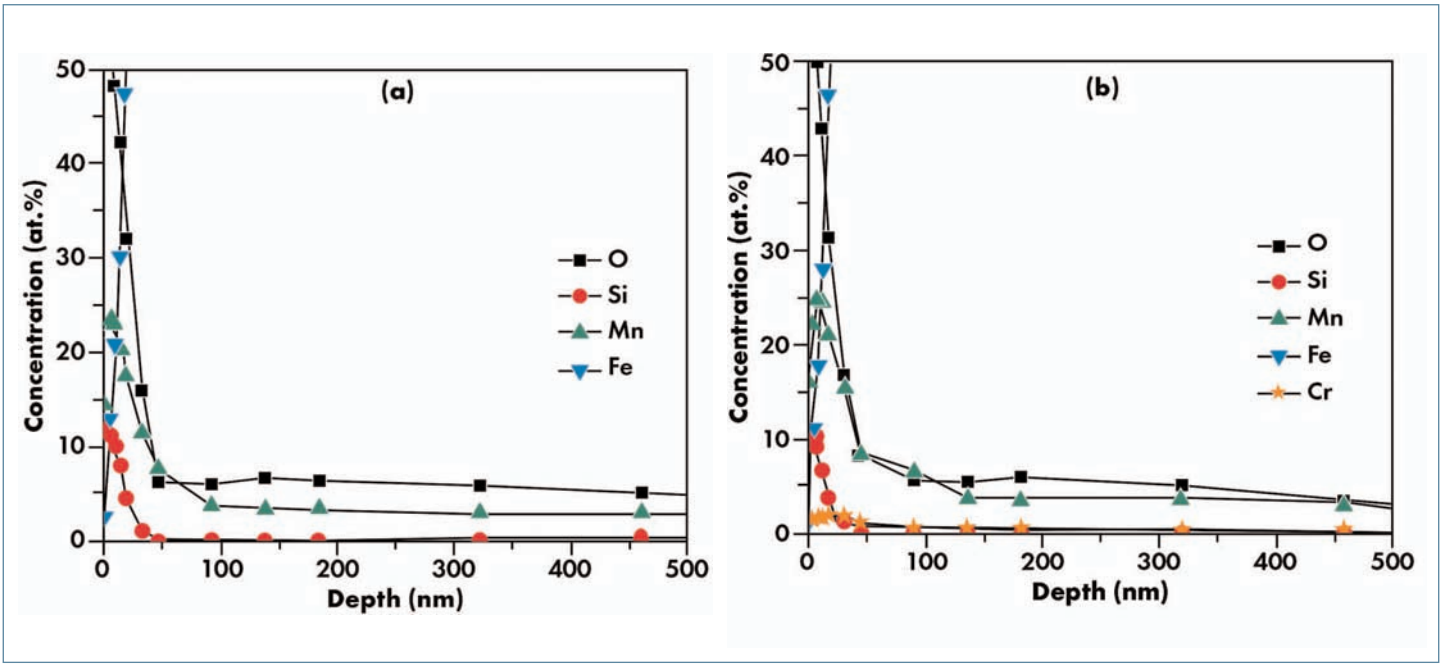

Fig 5: XPS depth profile of oxides formed on surface during annealing of (a) steel 1 and (b) steel 2.

Table 4. Identification of oxides on the steel surface using XPS .

Measured Binding Energies (eV) of Element						State (Compound)
Mn 2p3/2	Mn $2p_{1/2}$	Si 2p	Cr $2p_{3/2}$	Fe $2p_{3/2}$	O 1s	
641.6	653.4	103.4	576.5	706.6	530.4	MnO, SiO2, Mn2SiO4, Cr2O3 and Fe (metallic)

Table 5. Bare spot analysis of galvanized panels (total area analyzed: 8100mm²).

Sample No.	Average Bare Spot Size (mm2)	Total Bare Area (mm2)	Bare Spot (%)
steel 1	0.06	9.72	0.12
steel 2	0.10	13.77	0.17

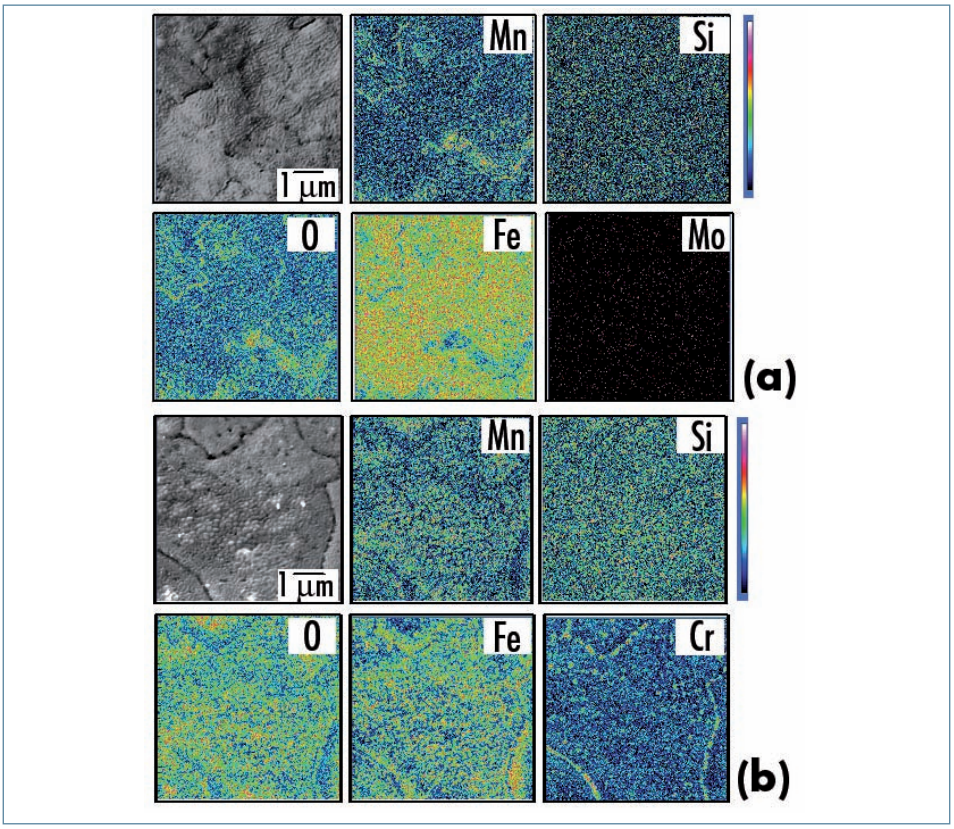

Fig 6: Elemental Auger maps of oxides formed on the surface during annealing of (a) steel 1 and (b) steel 2.

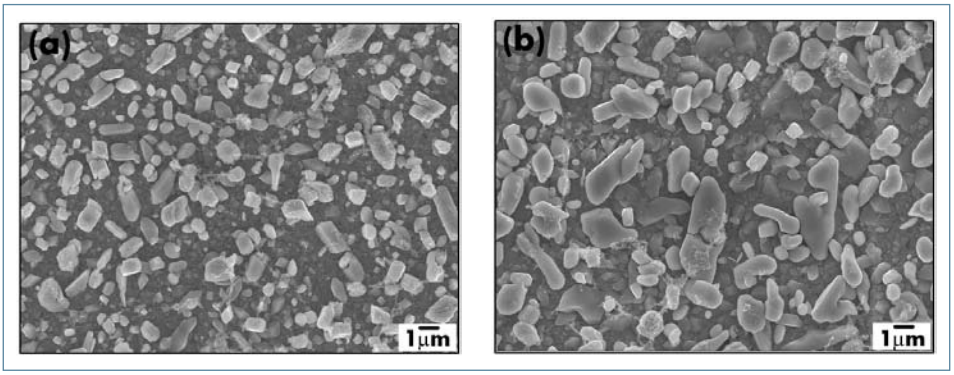

Fig 7: SEM micrographs of interfacial layer and Fe-Zn intermetallic phase after the Zn overlay was stripped with 10% H_2SO_4 in water (a) steel 1 and (b) steel 2.

demonstrated good wettability were stripped of their zinc overlay with 10% H_2SO_4 in water leaving any interfacial Fe–Zn and Fe–Al–Zn intermetallics intact. SEM micrographs of these samples are shown in Figure 7. Fe–Zn intermetallics were identified at the interfaces of both steels. Fe-Zn intermetallics should not be formed when galvanizing in a 0.18% dissolved aluminium containing zinc bath. Fe-Zn intermetallic phases typically form due to breakdown of the inhibition layer or can precipitate on the Fe-Al layer due to local Al depletion. Inhibition breakdown may have arisen from the heat generated during the austenite to bainite or martensite phase transformation, as elevated temperatures are known to promote this process [13]. The precipitation of Fe-Zn intermetallics may also have been promoted by aluminothermic reduction of surface oxides by the dissolved aluminium of the bath, causing local depletion of aluminium and promoting precipitation of Fe-Zn phases on the Fe-Al interfacial layer. In order to investigate the $Fe_2Al_{5-x}Zn_x$ ($0<x<1$) interfacial layer for both steels, a well wetted portion of the galvanized coating area was stripped with fuming HNO_3 leaving only the Fe-Zn-Al inhibition layer intact. Figure 8 shows the SEM micrographs of these samples. In general, a continuous $Fe_2Al_{5-x}Zn_x$ ($0<x<1$) layer was present for all samples, indicating complete reactive wetting and that the Fe-Zn intermetallics observed in Figure 7 precipitated on the surface of the Fe-Al layer due to local depletion of dissolved Al in the melt. From the above SEM micrographs it was also observed that the inhibition layer comprised two sub-layers: the lower sub-layer – next to the substrate surface – consisted of small, equiaxed crystals and the upper layer of coarse, elongated crystals [13,14].

Coating adherence with the steel substrate was determined by means of a 180° 'U' bend test per ASTM A 653/A 653M-09 [10]. The top surfaces of the 'U' bend test samples were analyzed using an optical stereoscope. Figure 9 shows the stereo-micrographs of the galvanized samples. It can be observed that aside from minor cracking of the galvanized coating, no flaking of the coating was observed and that, overall, the coating showed good adherence with the substrate steel.

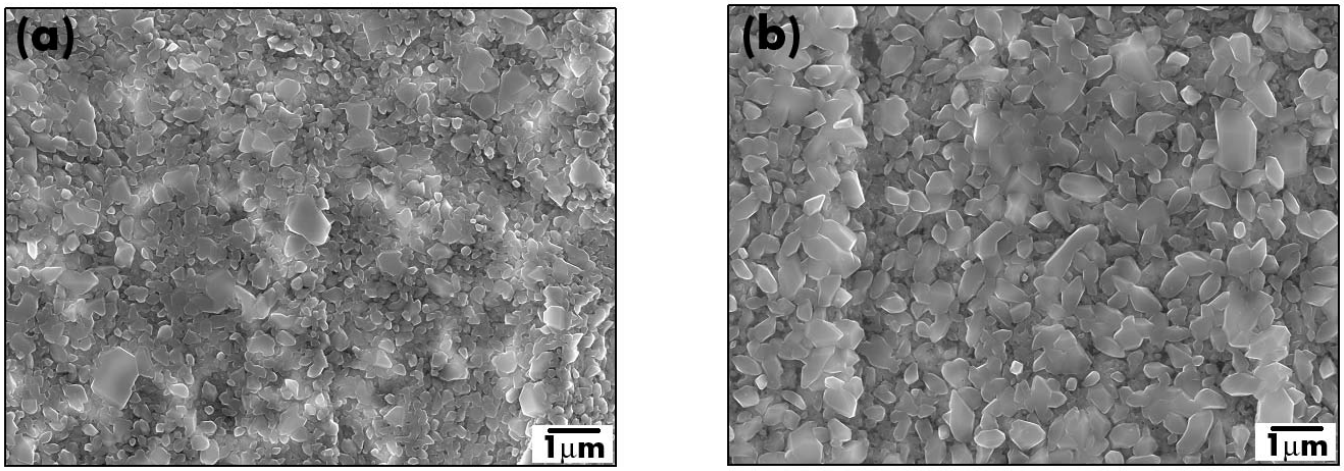

Fig 8: SEM micrographs of inhibition layer after the Zn overlay was stripped with fuming HNO_3 (a) steel 1 and (b) steel 2.

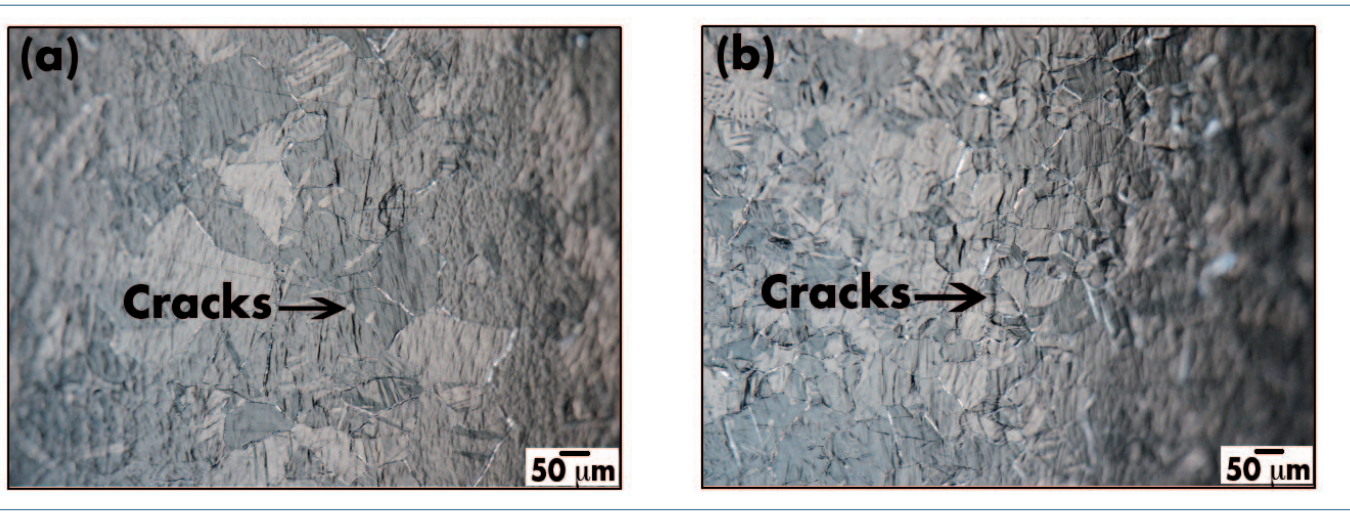

Fig 9: Stereo-micrographs of the top surface of 180° 'U' bend galvanized samples: (a) steel 1 and (b) steel 2.

CONCLUSIONS

The hot dip galvanizability of two laboratory-produced ultra high strength steels has been systematically analyzed to determine a suitable process window for CGL production. Microstructural characterization along with substrate mechanical properties as a function of thermal cycles based on their continuous cooling transformation behaviour was also determined. In the present case, the steels chemistries were designed around relatively lean compositions based on C, Mn and Si with additional hardenability being provided by Mo and Cr additions for steel 1 and steel 2, respectively.

For both steel compositions the target tensile strength of 1250 MPa (minimum) was achieved using austenitic annealing for 120s followed by cooling to room temperature at 50°C/s. It was also observed that when using similar cooling rates the Mo-containing alloy produced higher quench hardenability as compared to Cr alloy. For both the steels, surfaces which could be successfully reactively wet by the Zn(Al,Fe) bath were produced using a 95%N_2-5%H_2, -30°C dew point process atmosphere. From SEM, XPS and SAM analysis it was determined that oxides of Mn, Si and Cr formed during annealing and that these were distributed on the bulk grain surface as well as grain boundaries. There was no segregation and oxidation of Mo observed. However, these oxides did not have an adverse effect on the coatability, with both steels forming high quality, adherent coatings and a well developed Fe-Al interfacial layer. For both

steels, Fe-Zn intermetallics were also observed to have precipitated on the surface of the Fe-Al interfacial layer and may be due to the depletion of aluminium from the aluminothermic reduction of oxides on the steel surface during galvanizing. It can be concluded that for the above steel compositions, a suitable process window has been developed to produce galvanized ultra high strength (>1250MPa) martensitic and complex phase steels.

ACKNOWLEDGEMENTS

The authors would like to thank the members of the International Zinc Association Galvanized Autobody Partnership members, ArcelorMittal and the Natural Sciences and Engineering Research Council of Canada (NSERC) for their financial support of this research and the Materials Technology Laboratory, CANMET for the provision of the experimental materials through the RIEM program. The authors would also like to thank Dr. Li. Sun of ArcelorMittal (Dofasco) for XPS analysis, Shihong Xu of the Alberta Centre for Surface Engineering and Science for the Auger analysis and John Thomson, Mariana Budiman, Doug Culley and Steve Koprich of McMaster University for their technical support.

REFERENCES

[1] C. SCOTT, N. GUELTON, S. ALLAIN and M. FARAL, Mat. Sci. and Tech. Conf. Proc., Pittsburgh, USA, (2005), p 127.

[2] J. MAHIEU, S. CLAESSENS, B.C. DE COOMAN and F.E. GOODWIN, Galvatech'04, Conf. Proc., Chicago, USA, (2004), p 529.

[3] E.DE BRUYCKER, B.C. DE COOMAN and M. DE MEYER, Steel Res. Int. 75, 2, (2004), p 147.

[4] K.I. MATSUMURA, N. FUJITA and T. NONAKA, Galvatech'07, Conf. Proc., Osaka, Japan, (2007), p 392.

[5] E. C. OREN and F.E. GOODWIN, Galvatech'04, Conf. Proc., Chicago, USA, (2004), p. 737.

[6] M. BABBIT, Steel Res. Int., 77, 9-10, (2006), p 620.

[7] K.I. SUGIMOTO and B. YU, ISIJ Int., 45, 8, (2005), p 1194.

[8] J.R. MCDERMID, M.H. KAYE and W.T. THOMPSON, Met. Mat. Trans. B, 38B, (2007), p 215.

[9] Standard Test Method for Tension Testing of Metallic Materials, ASTM Standard, Designation: E 8/E 8M – 08

[10] Standard Specification for Steel Sheet, Zinc-Coated (Galvanized) or Zinc-Iron Alloy Coated (Galvannealed) by the Hot-Dip Process, ASTM Standard, Designation: A 653/A 653M – 09.

[11] E.M. BELLHOUSE and J.R. MCDERMID, Met. Mat. Trans. A, 41A, (2010), p 1539.

[12] R. KHONDKER, A. MERTENS and J.R. MCDERMID, Mat. Sci. Eng. A, 463, (2007), p 157.

[13] L. CHEN, R. FOURMENTIN and J.R. MCDERMID, Met. Mat. Trans. A, 39A, (2008), p 2128.

[14] E. BARIL and G.L'ESPERANCE, Met. Mat. Trans. A, 30A, (1999), p 68